



Pre-drill pore pressure prediction from 1D seismic velocity profile to 3D modeling using high resolution full waveform inversion velocity (FWI): deep water offshore, West Nile Delta

Maha Nabil El-Sayed Khattab ·

Nasser Mohamed Hassan Ali Abou Ashour ·

Abdel-khalek Mahmoud Mohamed El-Werr · Mai Fayek Mohamed Afifi

Received: 8 December 2021 / Accepted: 6 November 2022
© The Author(s) 2022

Abstract Pore pressure prediction is one of the most critical steps while planning new well delivery activity in exploration fields in order to achieve the well target by delivering a safe well. It is very important to understand the structural and stratigraphic complexity that may influence formation pressure differences in the study area. Also, it is critical to have a range of uncertainty in prediction to mitigate any kind of drilling problems and operational risks. In this case

study, the target is to predict the pore pressure gradient for four proposed exploration wells in West Nile Delta Raven field. The workflow has been applied utilizing tilted transverse isotropic seismic velocity and a high-resolution full waveform seismic inverted velocity. It is important as well to compare different methodologies where each one will have its own limitations. A manually picked normal compaction trend with the conventional Eaton pressure transform method was applied and compared with a BP internal normal compaction trend with a modified Eaton (Presgraf) pressure transform method in the Predrill prediction. The pre-drill pore pressure is finally compared with the actual measured pore pressure data that yields a good match.

M. N. E.-S. Khattab (✉)
BP Company, Cairo Festival City, Business Park D, Plot
#14 D03, Cairo 11477, Egypt
e-mail: maha.khattab92@yahoo.com; mahanabil_p@sci.asu.edu.eg

N. M. H. A. Abou Ashour
Emeritus Professor of geophysics, Geophysics Department,
Ain Shams University, Al-Khalifa Al-Mamoun, Abbasia,
Cairo - University Campus - College of Science,
Cairo 11566, Egypt
e-mail: naboashor@sci.asu.edu.eg; n_aboashor@yahoo.com

A. M. M. El-Werr
Professor of Seismic Methods, Geophysics Department,
Ain Shams University, Al-Khalifa Al-Mamoun, Abbasia,
Cairo - University Campus - College of Science,
Cairo 11566, Egypt
e-mail: aelwerr@sci.asu.edu.eg; aelwerr1@yahoo.com

M. F. M. Afifi
BP Company, Cairo Festival City, Business Park D, Plot
#14 D03, Cairo 11477, Egypt
e-mail: mai_afifi@yahoo.com

Article highlights

- Pore pressure prediction for the Nile Delta exploratory HPHT wells is critical.
- Pore pressure predicted using both conventional Eaton pressure transform, and modified Eaton (Presgraf) pressure transform methods.
- TTI and high resolution FWI seismic interval velocities were used to cover the prediction uncertainty.
- Seismic velocity shows the pore pressure ramp, but under predict the magnitude of the pore pressure gradient at problematic Messinian interval in the Nile delta basin.

Keywords Nile Delta · Pore pressure · PPFG · FWI · TTI · Eaton · Presgraf · Predrill

1 Introduction

Raven field is located 60 km offshore in the West Nile delta basin, where the water depth is between 500–700 m. The study area is approximately 500 km² as shown in the location map (Fig. 1).

The literature has mentioned several methods to predict over pressured intervals pre-drill using seismic velocity data (see Eaton 1975; Heppard and Albertin 1998; Badri et al. 2000; Carcione and Helle 2002; Sayers et al. 2002; Chopra and Huffman 2006; Sundaram and Jain 2008; Lu et al. 2009; Babu and Sircar 2011; Brahma et al. 2013; Karthikeyan et al. 2018; Das and Mukherjee 2020).

The Nile delta basin is not an active tectonic setting. The stress state in the Nile Delta area of interest is interpreted to be extensional in nature, with the post-Messinian sedimentary sequence ‘sliding

down’ into the Mediterranean basin on the near flat-lying Messinian evaporitic sequence, resulting in extensional faulting above the Messinian Evap./ Anhydritic limestone No salt diapirs, or associated stress rotations, are observed in the study area. Disequilibrium compaction is the main driver for the overpressure profile for the shales in the study area. The overburden section above the main Miocene-Langhian reservoir can be divided into three main stratigraphic sections Post Messinian, Messinian, and Pre-Messinian as per the Nile Delta Stratigraphic column (Fig. 2), where each section has its own geologic structural and stratigraphic complexity to be considered during pore pressure prediction as follows:

1.1 Post Messinian

The Pliocene—Pleistocene starts with a section in the field, which mainly consists of shale and sand sediments deposited in a middle to upper slope environment. This section is—characterized by:

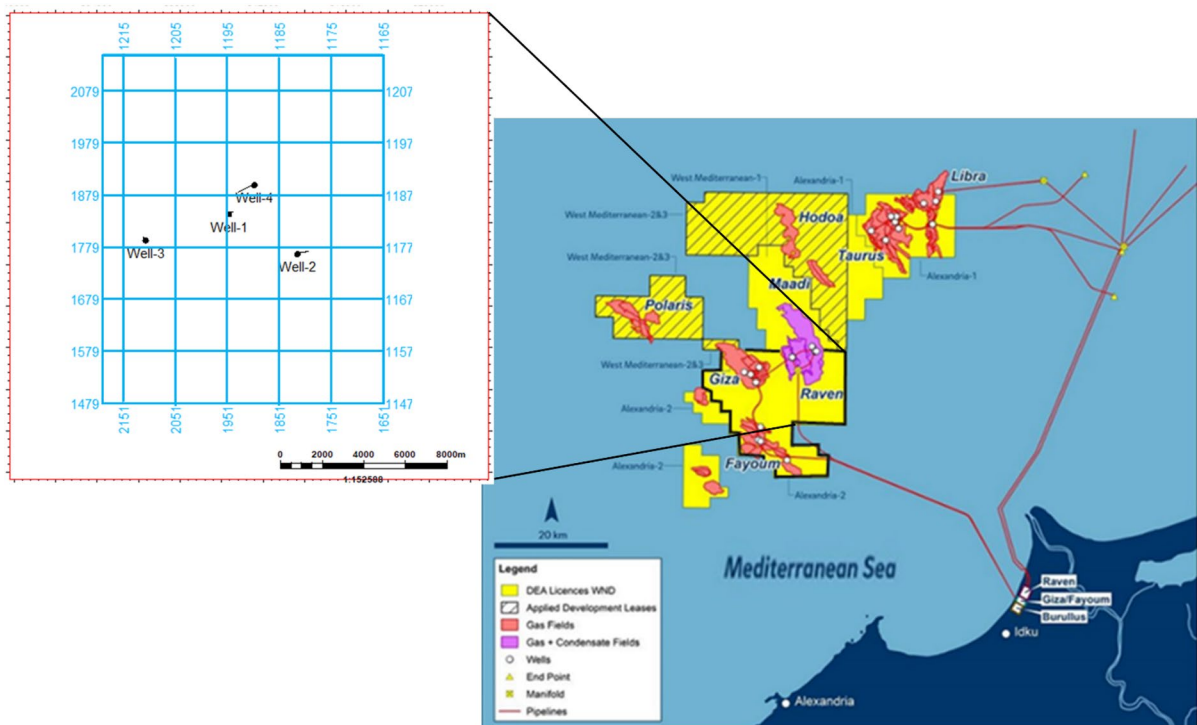


Fig. 1 Raven field—WND location map—Base map of the proposed exploration well locations

- Geobodies called mass transport complexes (MTCs) that consist of mixed shale and sand. Drilling MTCs might cause kicks due to the rapid deposition as a source of overpressure in isolated geobodies. From seismic data, MTCs can be easily identified due to their characteristically chaotic seismic character (Fig. 3a). The rapid sedimentation of recent sediments has resulted in overpressure in the Kafr el Sheikh (KFS) and the section below. In this section, wells must be sited as downdip as possible across these faults bounded permeable zones.
- High pressured, laterally extensive fairways above the Kafr el Sheikh formation (Fig. 3b) might cause pore pressure communication over long distances ranging from 5 to 20 km. The pressure in these extensive sands is limited by the fracture gradient of the sands further into the basin. If laterally connected, the resulting sand pressures may be below the shale pressure in the area of interest. If poorly connected, sand pressures are either at shale pressure, or depending on structural complexity, may show local lateral transfer. Detailed mapping and proper zonal isolation of these features is critical for this section to avoid drilling problems.
- Structural deformation represented by NE-SW trending normal faults that extend vertically from Pre Messinian to the seabed across the field are easily identified in seismic section (Fig. 3d).

1.2 Messinian

In general, the Messinian section sediments are deposited in fluvial/deltaic to sabkha and marginal marine environments (Kellner et al. 2018). At Raven, fluvial channels partly eroded the deposited Evaporitic/ anhydrite beds. The Messinian section is one of the problematic sections while drilling deep targeted wells in the Nile Delta. The early exploration/appraisal wells in the Nile Delta basin showed several pressure kick events turned into losses, resulting in sidetracking the wells, which added additional cost to the drilling operations. The complexity of this section is related to the preserved evaporite thickness (Evaporitic/Anhydritic limestone) and sometimes associated with Evaporitic/Anhydritic carbonates. These sediments are normally of very low porosity or permeability and

usually work as a strong seal trapping high pressure below. In seismic, the Messinian interval itself often looks low pressure because anhydrites, Evap./anhydritic limestone and carbonates tend to be very fast and hence result in a 'reduction' in pore pressure when converted from velocity to pressure. Seismic data resolution is critical in this section where the top of the Messinian unconformity surface in some areas is not resolvable because of the dramatic variation in Anhydrite distribution and thickness. This variation could mislead the pre-drill lithology prediction, which in turn could result in an unexpected kick while drilling (Fig. 3c). The sudden ramping up across the Messinian is driven by the fact that the presence of Evap./anhydritic limestone prevents the dewatering of the rocks below. When the Messinian anhydrites are less well developed, the ramp tends to be a little more gradual—but still there. It is important as well to adjust the well trajectory through this section to avoid drilling through fault tips or any congestion zones between antithetic faults (Fig. 3d). These zones tend to be structurally complex and may result in losses and wellbore stability issues.

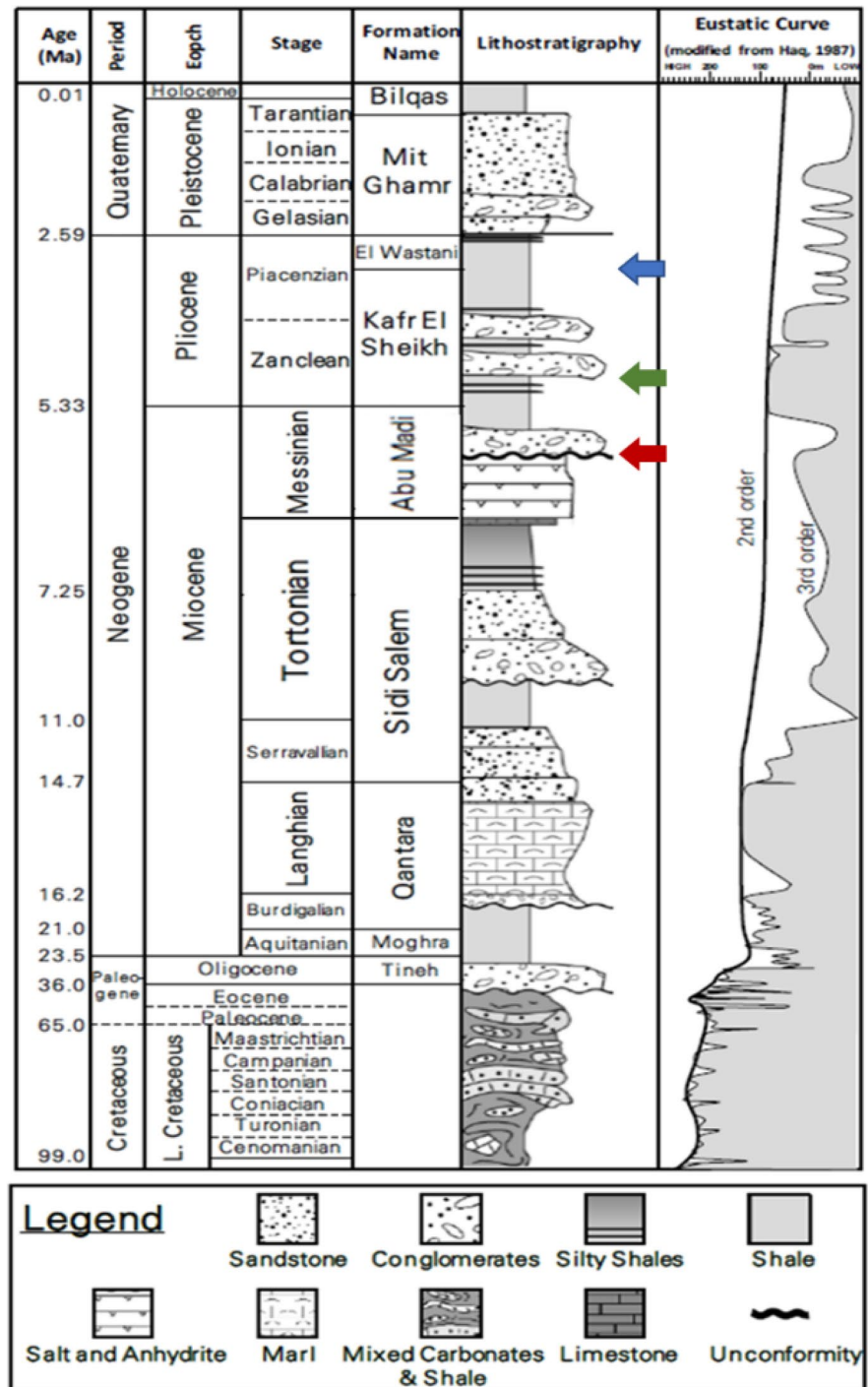
The Messinian Evap./anhydritic limestone beds are near horizontal and of few meters thickness trapping fluid (saline water) below but are not associated with notable stress changes across or around them. The nearshore part of the basin is extensional, and there are no indications of diapir formations, that could result in stress rotations around the structures.

1.3 Pre-Messinian

It is clear from seismic section (Fig. 3) that the entire Tortonian/Messinian succession has been eroded by compound unconformities (Kellner et al. 2018). The Late Serravallian to Early Tortonian is mainly characterized by a sand/shale section of fluvial channel systems across the field (Fig. 3e).

These channels extend far into the Mediterranean and pore pressure is limited by the fracture gradient of the sealing formations in the deep basin, therefore these channels tend to have lower pore pressure (regressed) with respect to the surrounding shales. These permeable zones (fluvial channels mostly) do not 'generate' pressure—they redistribute pressure. The overpressure is generated in the thick shale packages in the near shore section of the delta and is

Fig. 2 Stratigraphy of the Nile Delta (modified after Saleh 2018); where the blue, green and red arrows refer to the three expected over pressured intervals in the area



transferred through the sand channels into the Mediterranean to the North. Because these channels are so extensive and the overburden thins quite dramatically away from the Nile Delta mouth, the overpressure

generated nearshore reaches the fracture gradient of the overburden further into the Mediterranean and allows the overpressure to drain out. This means that nearshore, the sand overpressure is less than the

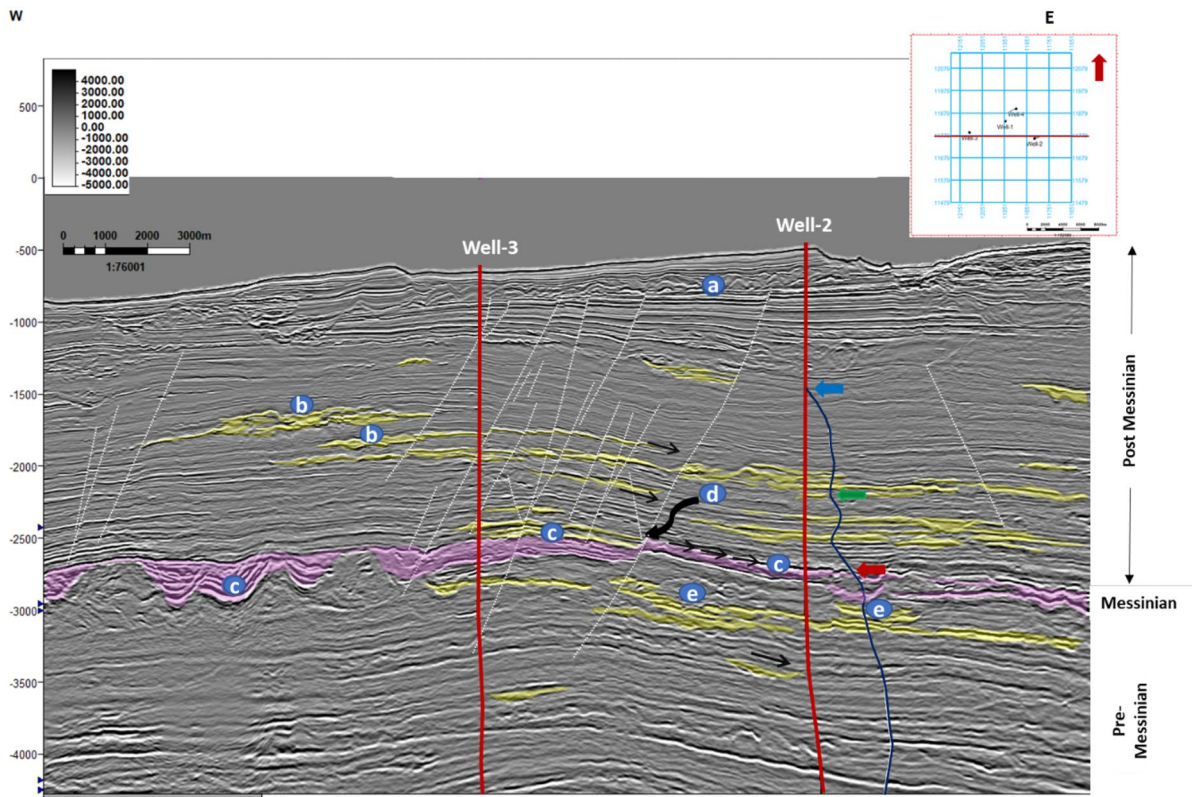


Fig. 3 E-W Full Offset Seismic Reflectivity Multi Azimuth Section in Depth Along the Proposed Locations for Well-2 and Well-3, Where: **a** on the section refers to a Plio-Pleistocene MTC, **b** highlights Pliocene channels, **c** highlights thickness and lithology variations of the Messinian erosion surface and **d** shows a fault congestion zone, **e** example of pre-Messinian fluvial channels, location map. The areas of sand facies within the fluvial channel systems are highlighted in yellow, areas

where there is a high probability to penetrate Evap./anhydritic limestone is annotated in pink color, black arrows are showing the dip direction of faulted beds and the well 2 prognosed location is at the downdip extension, dark blue curve to the right of well-2 is the projection of the prognosed pore pressure curve from the FWI velocity at well-2 location, and the blue, green and red arrows refer to the three expected pressure ramps in the area

shale overpressure and does not constitute an immediate drilling hazard. However, the associated problem with the lower pressured sands is that the sand fracture gradient is lower, which means that in these intervals with regressed sands, the drilling window is very narrow in some intervals, which may result in losses if the drilling mud weight is not optimized. There are two reason behind the lower fracture gradient in the pre-Messinian sands:

1. pressure regressions (due to extensive lateral distribution) resulting in a lower fracture gradient.
2. The lower stress ratio/K in sands compared to shales.

In other intervals, however, the sands are not as extensive and hence are at or near shale pressure. When drilled close to balance, this may result in connection gas events. The Qantara flooding event, deposited at the late Langhian due to the rise of sea level and is top sealing the main reservoir in the field at depth 5000 m tvdss, may show as a pressure ramp while drilling. Well-2 did not encounter any drilling issues while drilling this section

The available data in the Raven field study area are a 3D stacked, six azimuths seismic data volume and a high-resolution FWI velocity that can clearly image the geologic complexity in the Messinian and Post-Messinian sections.

In this study, TTI and high resolution FWI interval velocities were used to predict the pore pressure along four proposed high-pressure, high-temperature (HPHT) exploration wells. A manually defined normal compaction trend with the Eaton pressure transform equation and the BP internal Presgraf normal compaction trend with locally calibrated parameters and a modified Eaton (Presgraf) pressure transform methods for pore pressure prediction were applied to 1D seismic profiles. A 3D pore pressure cube using the FWI interval velocity was also built using the BP internal Presgraf algorithm. This 3D cube is used to highlight the higher risk, high pressure intervals that need to be avoided in the planning phase of the four proposed exploration wells to mitigate the risk to drilling operations.

2 Methodology

2.1 FWI velocity

- (a) An initial velocity model was built using the velocity measurements within thirteen wells across the field.
- (b) Velocity interpolation between wells and extrapolation away from the control points guided by the structural framework horizons.
- (c) The anisotropic parameters β : the tilt angle of the polar axis, V_{po} : the interval velocity, and the Thomsen parameters ϵ and δ (Thomsen 1986) have been estimated.
- (d) Two tomographic iterations were applied for velocity model update. In each iteration the flattening of the CIPs (Common images point) gathers were used to quality assurance and quality control the output. The tomographic process was applied in the depth domain. At this stage in the workflow the target was to create a suitable (initial) model to use as the starting velocity for the full waveform inverted velocity (FWI) process.
- (e) Shot gathers forward model (synthetics) using the initial Tilted Transverse Isotropic (TTI) tomographic interval velocity (Fig. 4a) as an input for the FWI velocity model building were obtained. If this initial model is very far from “reality”, FWI will not be successful in properly updating

the velocity. Hence, a reasonable realistic initial FWI model was built.

- (f) Inversion process is translated through the objective function required to minimize the mismatch between the modeled (synthetics) data and observed (real seismic) data.
- (g) The residuals between the shot gather forward modeled data and the observed data were calculated.
- (h) The final step was to apply the mismatch and update the FWI interval velocity model (Fig. 4b).

A depth difference of approximately 100 m (328 ft) at the onset of the lower velocity interval was observed between TTI and FWI velocity sections at Messinian interval where, on FWI data it is thinner by ~ 40 m TVT and deeper by the 100 m at well-2 proposed location compared to the TTI seismic velocity. This thickness and depth variation change across the field can introduce uncertainty in the Messinian ramp onset depth, magnitude and possibly the steepness from one dataset to another. To cover the depth uncertainty both velocity cubes were considered to predict the pore pressure envelope before drilling.

2.2 1D pore pressure prediction

In this study, two types of updated pre-stack depth migration (PSDM) seismic velocities were very useful and gave reliable details for the pre-drill pore pressure prediction using (1) a manually picked normal compaction trend with the conventional Eaton pressure transform method and (2) a BP internal Presgraf normal compaction trend with a modified Eaton (Presgraf) pressure transform method, as explained in the following steps:

- (a) Interval seismic velocity profiles were extracted every 1 m along the 4 proposed well locations from both the TTI and FWI seismic velocities. By plotting the interval velocity profiles in ft/s on a normal scale versus the true vertical depth (TVD) in ft (Fig. 5) the relation at well-2 location shows:

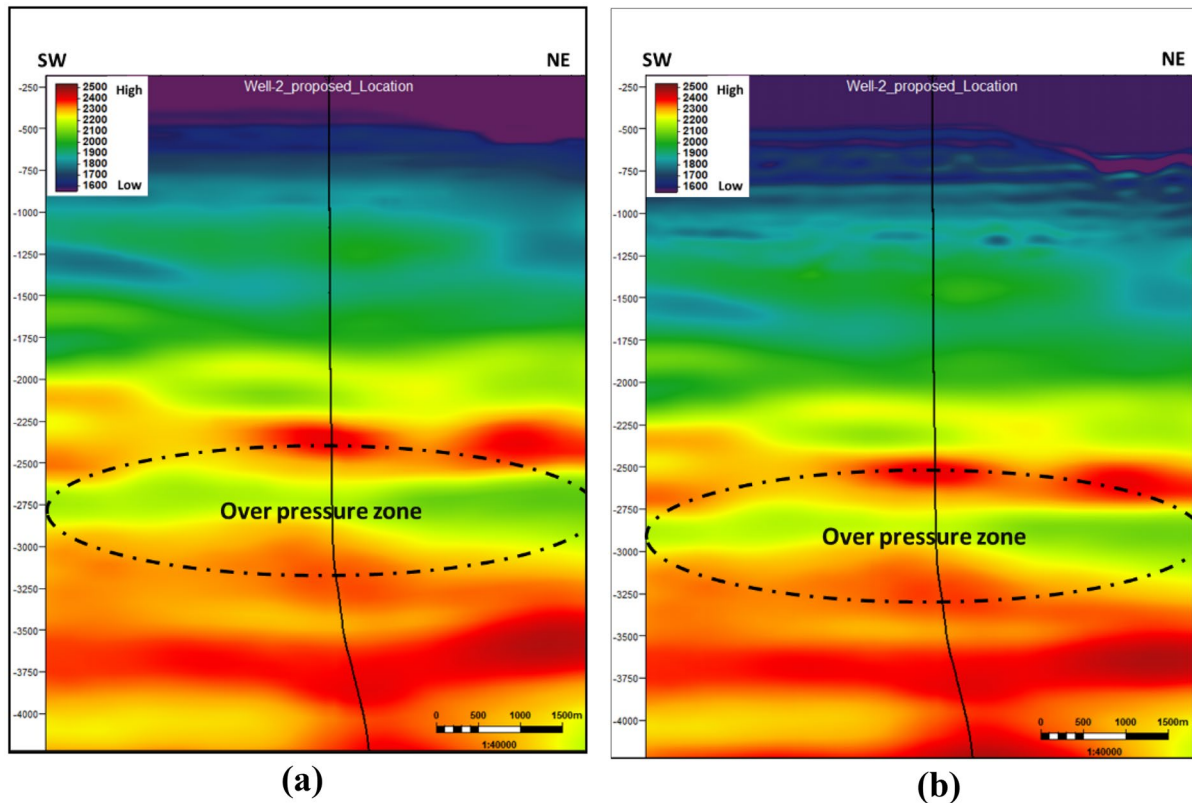


Fig. 4 seismic well section along proposed well-2 location showing TTI (a) and FWI (b) seismic interval velocity in depth domain

- Increase in velocity with depth following the hydrostatic pressure regime in the shallow section from 1000 ft down to ~4000 ft.
- A pressure increase at top of Kafr el Sheikh (KFS) formation represented by a decrease in the interval velocity between ~4200 and 6000 ft on the TTI and 4656–6656 ft on the FWI interval velocity profiles (Fig. 5), where the FWI was predicting the over-pressured zones ~200 m deeper than the TTI seismic velocity.
- The blue arrow refers to the top of the over-pressured zone where the interval velocity starts to decline from the hydrostatic trend.
- The velocity profile along the proposed location for well-2 shows a possible over-pressured zone at a depth of ~6500 ft on TTI and ~7200 ft on FWI (green arrows, Fig. 5).
- A pressure increase was clear at the Messinian at a depth of ~7750 ft from TTI Seismic

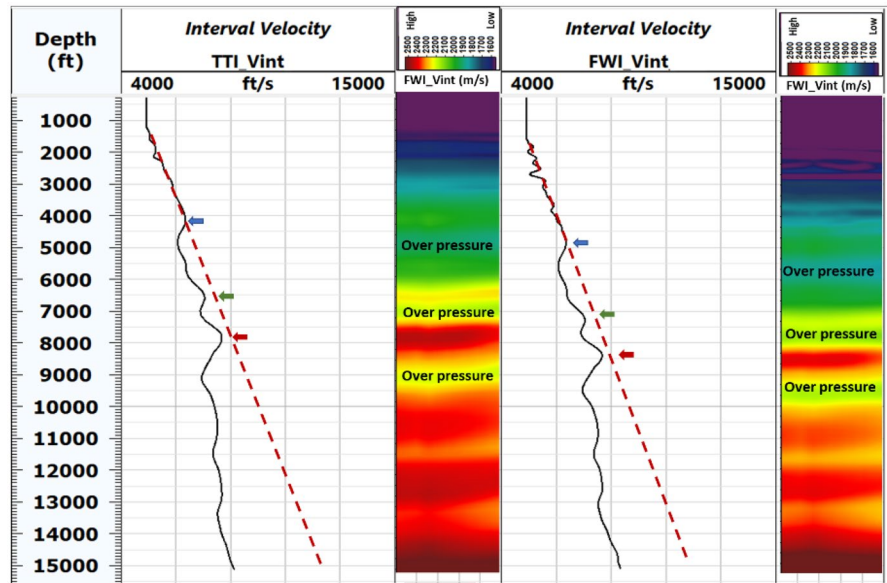
Velocity and ~8420 ft from FWI velocity (red arrows, Fig. 5).

- Both FWI and TTI seismic velocities were observed to be dominated by the lithology and rock compaction at the deep reservoir interval, where both datasets appeared to be smoothed and failed to reflect the gas response at the expected reservoir section between (14,200–14,650 ft).

- (b) Interval transit time (Δt) in ($\mu\text{s}/\text{ft}$), which is a porosity-dependent parameter (i.e., increases with increasing porosity) can be calculated from seismic interval velocities in (m/s) across the study area applying the following equation (Hottman and Johnson 1965):

$$\Delta t(\mu\text{s}/\text{ft}) = \frac{0.3048 \times 10^6}{V_{int}} \quad (1)$$

Fig. 5 Well-2 interval velocity profiles and seismic velocity display extracted along—proposed well location- 2 from the FWI and TTI seismic velocities versus TVD depth and the manually defined normal velocity trendline (Red dashed line)



- The interval transit time profiles calculated from interval seismic velocities are plotted against TVD depths in ft.
- This plot is used for marking the onset of the over-pressured zones, where the transit times increase with depth (Fig. 6) in the same intervals that showed a decrease in the previous interval velocity plots (Fig. 5).
- There is no increase in slowness reflecting gas response as expected from the smeared interval velocity response at the prognosed reservoir section between 14,200 and 14,650 ft.
- This plot is also used to estimate the normal compaction trendline that is used for the calculation of the normal pore pressure gradient. The normal compaction trendline can be estimated using the slope of the slowness line in the interval interpreted as normally compacted (e.g., from ~1000 to 4000 ft in Fig. 6). The risk is that the shallow sediments in this interval are already over pressured, and the slope is not fully indicative of normal hydrostatic pressure, so calibration is generally required.

$$\begin{aligned} \text{Normal hydrostatic trend (us/ft)} \\ = \text{slope} * \text{depth(ft)} \end{aligned} \quad (2)$$

- (c) The bulk density (ρ_b), which depends on porosity, matrix type, matrix density, fluid type and fluid density can be estimated either in terms of interval velocities using (ENI 1999) formula:

$$\rho_{b,i} = \rho_{mat} - (1.228 * (\rho_{mat} - \rho_f)) \times \left(\frac{1 - \frac{V_{int,i}}{V_{mat}}}{1 + \frac{V_{int,i}}{V_{mat}}} \right) \quad (3)$$

where (ρ_{mat}) is the density of the rock matrix 2.66g/cc, (ρ_f) is the density of the rock fluid 1.01 g/cc for water and 0.69 g/cc for gas (these values are defined for the study area and will be different per area), ($V_{int,i}$) and (V_{mat}) are the interval and matrix velocities of the formation(m/s), (ρ_{mat}) is the density of rock matrix 2.66 g/cc.

Or it can be estimated utilizing the interval transit time profile calculated from seismic at the proposed well location by applying the following formula (Bellotti and Giacca 1978) which requires an initial lithology prognosis along the proposed well location from the seismic data observations and geologic understanding in the study area.

$$\rho_b = \rho_{mat} - \left((1.228 * (\rho_{mat} - \rho_f)) \times \left(\frac{\Delta T_{log} - \Delta T_{mat}}{\Delta T_{log} + \Delta T_f} \right) \right) \quad (4)$$

where (ΔT_{Log}) is the interval transit time calculated from seismic interval velocity along the proposed

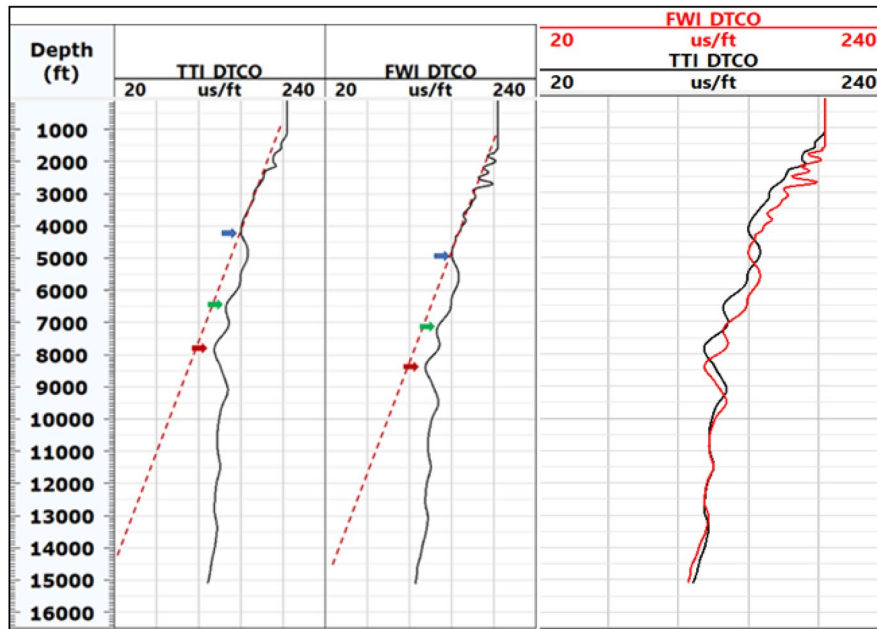


Fig. 6 Interval transit time profiles calculated from the FWI and TTI seismic interval velocity versus TVD depth in ft along the proposed well-2 location. The normal compaction trendline (Red dashed line), representing the slowness expected for normally compacted (hydrostatic) overburden, and the slope of the

trendline in the four proposed well locations ranged between 0.4 and 0.6 $\mu\text{s}/\text{ft}^2$. Arrows indicated the onset of the high transit time intervals (over-pressured zones). The third track compares the TTI versus FWI estimated interval transit time from the seismic interval velocities for proposed well-2 location

well location, (ΔT_{mat}) and (ΔT_f) are the interval transit time in the rock matrix and fluid ($\mu\text{s}/\text{ft}$).

- The interval transit time values used in the study are shown in (Table 1) and are based on a lithology prognosis at each proposed well location based on familiarity with the geologic deposition in the study area. For example, a distinctive appearance of the seismic amplitude with high impedance reflects the top of Messinian erosion surface in the field.

Gardner empirical Eq. (5) was used as well to predict the pseudo ρ_b that was less than the outcome ρ_b predicted from Bellotti and Giacca (1978) Eq. (4) by a max difference of ~ 0.1 g/cc and this means less estimated overburden stress and less pore pressure prediction and failed to reflect the deep reservoir section.

$$\rho_b = 0.31 \times V_p^{0.25} \quad (5)$$

- The seismic velocity failed to reflect the gas content which impacted the calculated interval slowness (DTCO) across the expected reservoir interval. Bellotti and Giacca (1978) Eq. (4) was used to obtain pseudo bulk density ρ_b log along proposed well location and it showed a good prediction for the sands in the shallow section but, there was a limitation to predict correct ρ_b values within the expected reservoir interval, where the calculated density at the reservoir section was higher compared to the overburden section.
- These density variations between the two equations are expected to have a minor impact on the final pore pressure prediction.
- Calculated bulk density using Eqs. (4) and (5) in g/cc, plotted versus TVD depth in ft (Fig. 7).

- (d) The overburden pressure (σ_{ovb}), or vertical stress, is calculated in *psi* (Fig. 8) as follows:

Table 1 Average interval transit times for different matrix types and fluids in the study area after (Bourgoyne et al. 1991)

Formation	$\Delta t_{mat} (\mu S/ft^{-1})$
Sandstone	53
Limestone	47.6
Clay/Shale	62.5
Anhydrite	50
Fluids	$\Delta t_f (\mu S/ft^{-1})$
Saline water	189
Brackish water	200
Fresh water	218
Gas	626

$$P_{ovb} = \sum_{i=1}^N P_{ovb,i} = \int_i^N 0.43346 \cdot \rho_{b,i} \cdot dD \quad (6)$$

where: (D) is the TVD depth of interest in ft.

(e) Finally, pore pressure can be predicted using the ‘observed’ and ‘normal’ velocity by applying Eaton’s equation, as follows:

$$P_P = P_{ovb} - (P_{ovb} - P_{pnormal}) \cdot \left(\frac{V_{observed}}{V_{normal}} \right)^3 \quad (7)$$

where: $P_{pnormal}$ is the normal hydrostatic pressure. ($V_{observed}$) is the observed interval velocity of the formation in (ft/s) and (V_{normal}) is the velocity that would be expected if the rocks were normally compacted in (ft/s). Assuming a sea water density of 1.033 g/cc and a normal hydrostatic gradient of 0.4378 psi/ft (equating to formation water density of 1.01 g/cc) to calculate the $P_{pnormal}$.

The PRESGRAF Amoco overburden, normal compaction trend and pressure transform models, developed by Martin Traugott (Heppard et al. 1998), were used as another tool to predict pore pressure. The Presgraf model is based on a global database and has a generic definition of how rocks are expected to compact with depth. It allows for trendline calibration and adjustment of the parameters for different formations based on local calibration. The Presgraf method inherently applies a generic mean stress calculation for a ‘normally stressed environment’ with empirically based assumptions on the relationship between S_v , SH_{max} and SH_{min} .

The methodology applied when using the conventional Eaton pressure transform is based on

interpreter definition of the normal compaction trend for the individual datasets (Fig. 9) and uses S_v rather than mean stress to calculate pore pressure.

Pore pressure predicted for the shallow section using the TTI velocity showed a wide range of uncertainty between the two different methodologies, where the observed difference was 2 ppg at depth of 5000 ft and 1 ppg at depth of 8000 ft. The FWI prediction showed a narrower range of uncertainty as the observed difference was 1.3 ppg at depth of 5000 ft and no difference at depth of 8000 ft. TTI showed a difference of 0.3 ppg while FWI showed a difference of 0.5 ppg at the Messinian problematic zone. Along the pre-Messinian section between 10,000 ft down to 15,000 ft, TTI showed identical prediction from both methodologies while FWI showed a consistent range of uncertainty ~ 1 PPG.

The differences using both methods is mainly the result of the difference in the normal compaction trend definition. The applied ‘Eaton’ methodology used a manually defined Normal Compaction Trend (NCT), which is subject to interpreter judgement to select where to deviate from the hydrostatic pressure. The Presgraf normal compaction trend defines the NCT based on generic rock compaction assumptions that can be and have been calibrated to regional analogues (Fig. 10).

Having a range in the prediction methodologies is important to cover the uncertainty range, especially for safe delivery of the first exploration wells in the area. By drilling more wells in the field, the actual data will be useful for more accurate calibration to allow for reducing the uncertainty in the predrill predictions for future wells.

Fig. 7 A comparison between the calculated bulk density profiles for FWI and TTI seismic velocities by applying Gardner, Bellotti and Giacca (labelled 'B&G') equations, where arrows refer to onsets of pre-defined high-pressure zones along the proposed well-2 location

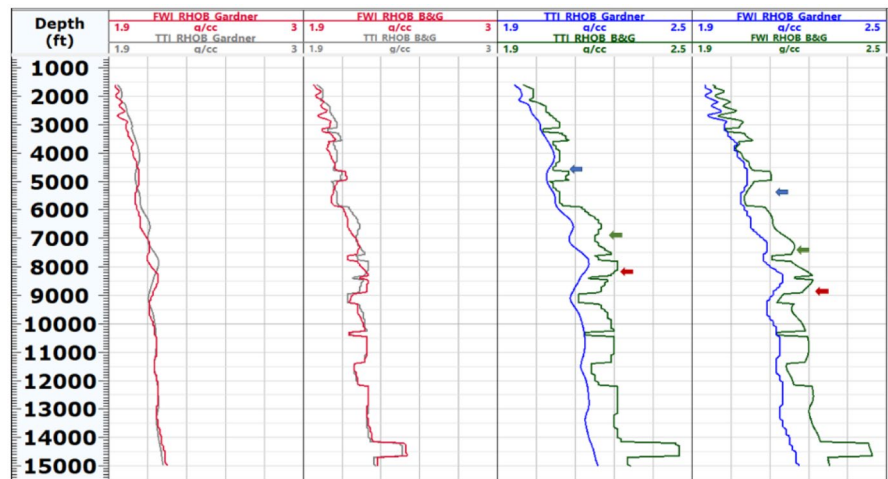
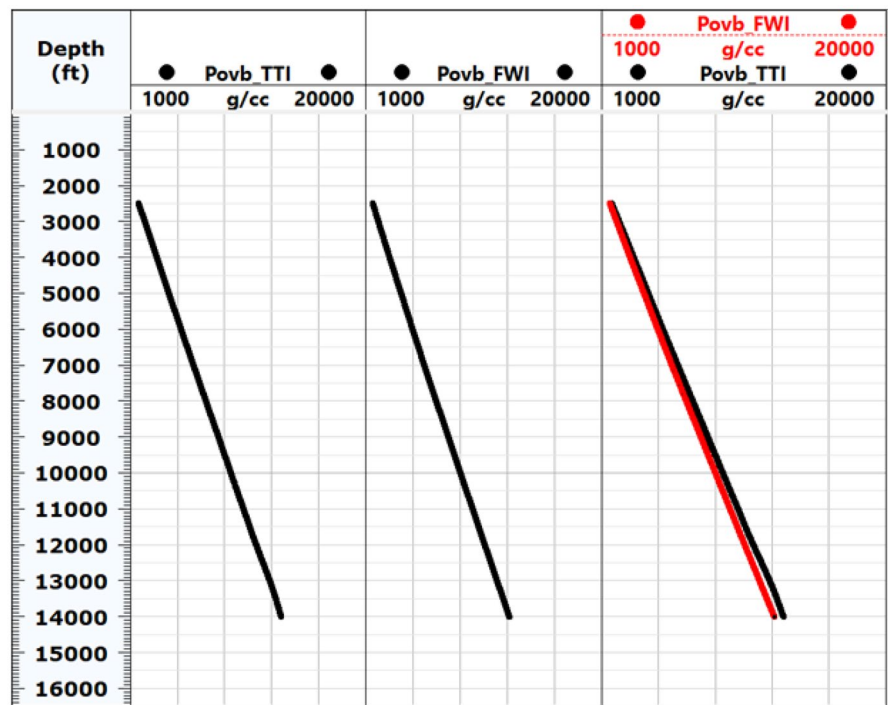


Fig. 8 Calculated overburden pressure in Psi for FWI and TTI seismic velocities plotted versus TVD depth along the proposed well-2 proposed location, the third track compares the TTI vs FWI estimated overburden pressure curves



2.3 3D pore pressure cube

In this study a 3D pore pressure cube was also generated to be used to identify the regional pressure regimes over the field and to check the well placement locations relative to the over-pressured intervals (e.g., KFS and Messinian).

A 3D pore pressure cube was built for the Raven field using the Presgraf normal compaction trend

and pressure conversion, utilizing the high resolution FWI seismic velocity. Assuming a sea water density of 1.03 g/cc, normal hydrostatic gradient of 0.4378 m/ft, formation water density of 1.01 g/cc, average volume of clay (V_{CL}) of 0.45 for and compaction factor of 5700 across the area.

A 2D pore pressure map extracted as an example at the top of the over-pressured Messinian interval was integrated with the geologic understanding and

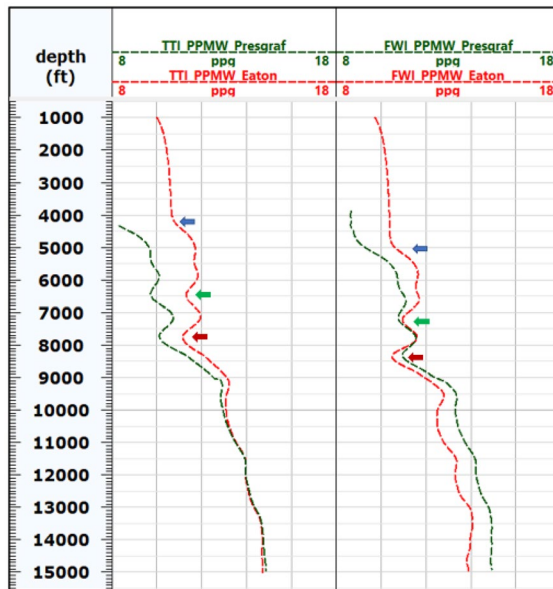
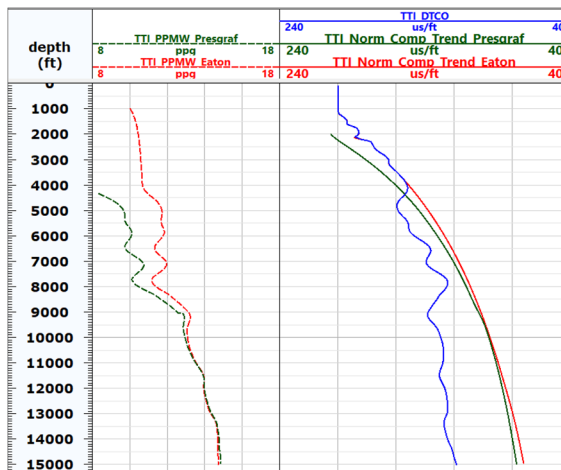
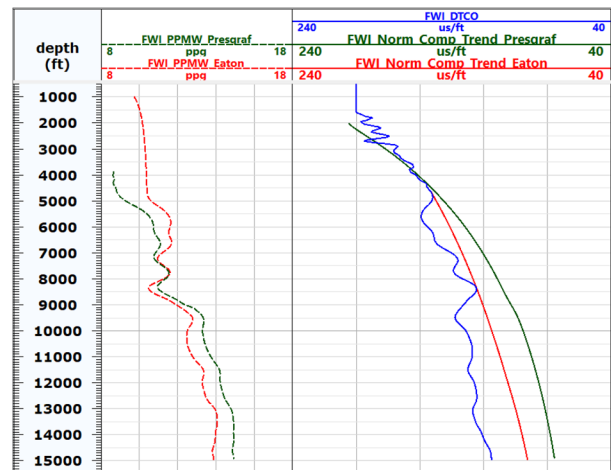


Fig. 9 Shows the pore pressure calculated using the manually defined normal compaction trend and the Eaton pressure transform equation (red, labelled ‘Eaton’) and the results from the Presgraf normal compaction trend and pressure transform (green, labelled ‘Presgraf’), assuming a sea water density of 1.033 g/cc, Formation water density of 1.01 g/cc, volume of clay (V_{CL}) of 0.5 for post Messinian section and 0.45 for Pre-Messinian section and compaction factor of 5700



(a)



(b)

Fig. 10 Showing the NCT manually defined in Eaton Method versus the defined Presgraf trend which is calibrated to regional analogues for TTI and FWI datasets at the proposed well-2, where the manually picked trendline is the solid red-labelled ‘Eaton’ and the trendline generated by Presgraf based

colored to reflect the relative pore pressure related risk across the field. The 2D map (Fig. 11) shows the four well locations optimized to drill this problematic interval in a relatively low to moderate pore pressure risk zone, allowing them to be drilled with manageable drilling mud weights.

Well trajectory optimization in this field is not only controlled by avoiding over-pressured areas in the shallow section. In some wells the decision will be made to drill through an over-pressured area in the shallow section with pre-drill mitigation plans not to compromise the well’s target location.

3 Validation of pre-drill versus post-drill pore pressure

A comparison between the pre-drill predicted parameters and the actual measured values were established. The plot below (Fig. 12) shows that the calculated interval transit time from FWI and TTI seismic velocities along well-2 only reflects the general trend while it is missing the details seen in the higher resolution sonic log data and as mentioned before it failed to predict the discovered reservoir.

on the global analogues database is the Solid green- labelled ‘Presgraf’. The trendlines are giving explanation for the observed uncertainty differences in pore pressure prediction between both datasets and methods

The same comparison between the pre-drill estimated bulk density from seismic data and the bulk density logs is shown in Fig. 13.

Overall velocity derived densities appeared to be too low which would have underestimated the overburden compared to actual overburden pressure or stress. Shale bulk density calculated using Gardner equation was less than the actual shale density logged post drilling the well although it gives reasonable results at the reservoir section by reflecting the velocity response. On the other hand, Bellotti and Giacca (1978) equation (4) showed a relative better prediction for sand and shale in the overburden section but, was underestimating the bulk density compared to the actual (RHOB) log, and completely failed to predict the reservoir section prediction.

Underestimating the bulk density (RHOB) leads to an underestimated overburden stress, which translates directly to an equal underestimation of pore pressure when using the Presgraf or Eaton pressure transform equations. Pre-drill lithology prediction from seismic data carries an uncertainty that requires:

- Calibration of the seismic velocity with the exploration wells outcomes, especially across the reservoir section.
- Running a post drilling formation evaluation study to modify the average ΔT_{mat} and ΔT_f values (Table 1) for better prediction using Bellotti and Giacca (1978) equation in future well predictions.
- Calibration of the Gardner equation constants.
- Acquiring shallow density measurement in order to calibrate the shallow section with real data for better future PP prediction.

Finally, the pore pressure gradient prediction from the two models tested using both seismic velocities is compared versus the actual pore pressure gradient (Fig. 14). The pre-drill model using the regionally calibrated Presgraf normal compaction trend and pressure transform model shows a good match between the pre-drill estimates and the actual pore pressure gradient. Due to the early onset of overpressure, it is difficult to manually define the normally pressured section and identify exactly what is the onset of overpressure.

Of note also is the fact that both pre-drill pressure prediction methodologies fail to fully define

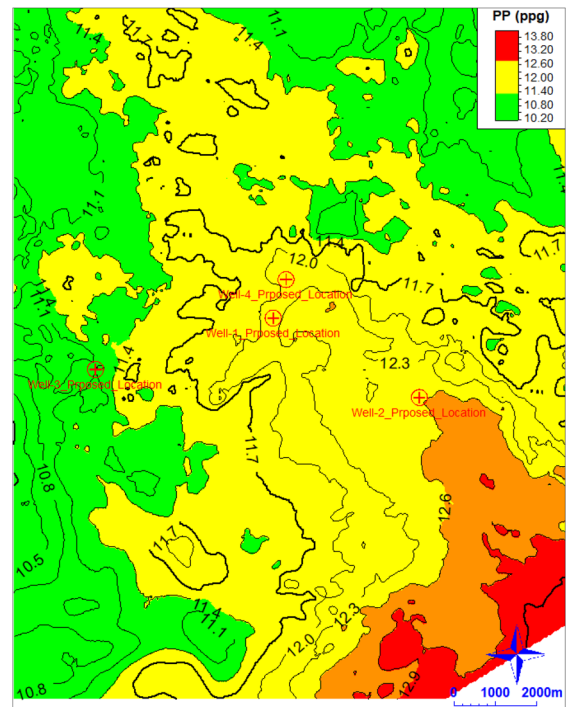


Fig. 11 A pore pressure gradient map extracted on top Messinian (most critical zone while drilling the Nile Delta deep wells) showing the 4 proposed well locations optimized in relatively low to moderate risk locations

the Messinian pressure ramp magnitude. The FWI data with the Presgraf approach shows the closest fit where it succeeded in the onset and ramp magnitude prediction down to depth of 8750 ft, but still underestimates the actual pressure at the maximum peak of the ramp by 0.3 ppg and predicted the maximum peak deeper than actual.

On the other hand, the TTI with the Eaton approach could predict the depth of the maximum peak of the ramp, but still underestimates the actual pressure at the maximum peak of the ramp by 0.5 ppg and also failed to predict the onset and the magnitude of the ramp down from it, which is mostly due to the fact that the Messinian consists of a range of lithologies that are generally very fast (Anhydrite and Carbonates) and as such mask the slower velocities associated with overpressure in shales. Equally, the velocity data are not able to match the severity (or steepness) of the ramp, which is about 1.5 ppg over ~ 500 ft. This is driven by the limitations on frequency content. Although the FWI is of a higher resolution

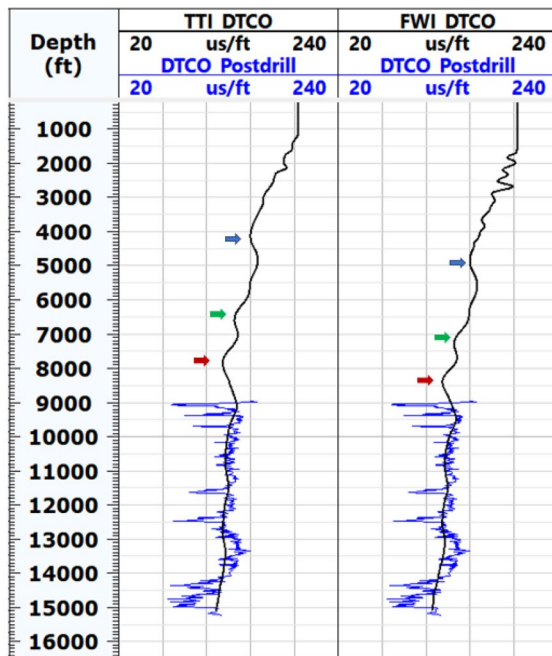


Fig. 12 Calculated interval transit time pre-drill (black curve) from FWI and TTI seismic velocities and the actual interval transit (DTCO) log data (Blue Curve) acquired post drilling well-2 plotted versus TVD depth

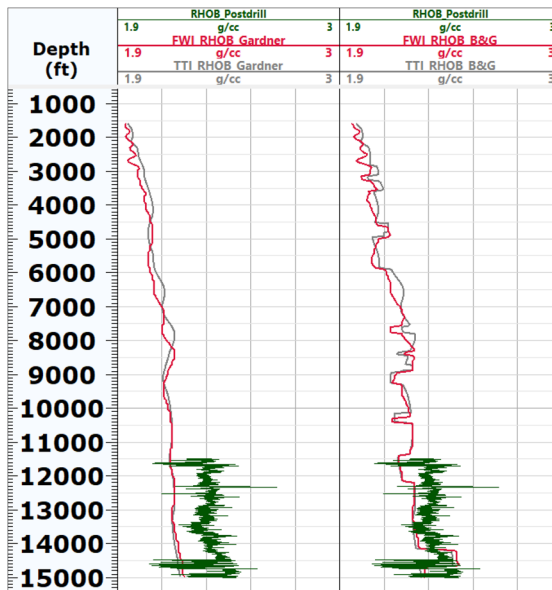


Fig. 13 Calculated bulk density from FWI and TTI velocities using Gardner equation (Red curve) and (Grey curve) using Bellotti and Giacca (B&G) equation versus the bulk density (RHOB) log data (green curve) post drilling well-2

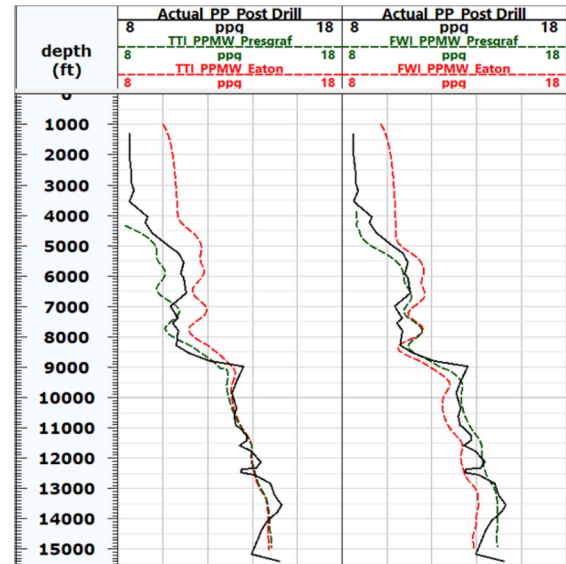


Fig. 14 Calculated pre-drill pressure gradients in ppg using Eaton (red curve) Presgraf (green curve) in ppg using the FWI and TTI seismic velocities compared to the actual post-drill pressure gradient (black curve) for well-2 plotted versus TVD depth

compared to the TTI velocity, its dominant frequency content is still less than 10 HZ, which is not sufficient to detect the details or the exact magnitude of the ramp. It is recommended to calibrate the base of the Messinian section across in the FWI model using the post drilling results from the four exploration wells in order to improve the predictability of the maximum peak of the ramp for future development wells.

4 Summary and conclusion

The Raven field study area is located in the offshore West Nile Delta basin. The objective of this study was to predict the pre-drill pore pressure utilizing TTI and high resolution FWI seismic velocities. To cover the depth uncertainty of the overpressure onsets both velocities were considered. FWI pre-drill seismic velocity identified the onset depth of the overpressure intervals deeper than the TTI prediction by approximately 100 m at well-2 location and the thickness of the Messinian interval was thinner by ~ 40 m TVT.

Two approaches to defining a normal compaction trend (manual and Presgraf model) were used as well as two different pressure transform models (Eaton and

Presgraf) were applied, where Eaton was used with the manually defined NCT and Presgraf transform model with the Presgraf NCT. Normal compaction trend definition has the most impact in pore pressure prediction calculation. Calibrating all inputs to the pre-drill prediction algorithms (i.e., Sonic, density, Gardner equation terms, etc.) with the real data collected in the exploration wells is highly recommended for better prediction along development wells. The pre-drill prediction using the Presgraf algorithm has shown a good match between the pre-drill pore pressure gradient estimates and the actual pore pressure gradient more than the Eaton approach.

The workflow started with 1D seismic velocity profiles at the proposed well locations transforming it into 1D pore pressure profiles. A 3D pore pressure model for the entire field was built in order to highlight the areas of potential high operational risk and to optimize the well trajectories and the risk mitigation plan. The Messinian in this field is a problematic interval with a steep and sharp ramp. Although the FWI seismic velocity is of a higher resolution compared to the TTI velocity both are 'smeared' over the Messinian interval. Both seismic velocities were capable of showing the pore pressure ramp, but both TTI and FWI seismic velocities under predict the magnitude of the pore pressure gradient at this critical interval, which requires vigilance while drilling.

Acknowledgements I am grateful to all specialists who gave of their time and expertise to contribute, edit, revise and technically assure this work: Martin L. Albertin (ex- SETA- PPF, BP), Buis-Wegerif, Juliette (Pore Pressure Advisor, BP), Sam Buist (Geophysicist, BP), Ahmed I. Abushady (PPF Special-ist, BP), Mark A. Benson (ex- Seismic Processor, BP), Bertram Nolte (ex- Seismic Processor, BP), Dr. Ahmed El-Bassiony (Seismic data processing administrator, Ain Shams University), Shweta Sangewar (Geophysicist, BP), Amin Moursy (Senior Geologist, BP), Mohamed Mahdy (Geophysicist, BP), Ahmed Mamdouh (ex- Data Management team contractor, BP), Tim Fennah (Senior Geophysicist, BP).

Author contribution MK: Conceptualization, Data curation, Writing- Original draft preparation, Editing and Software. Emeritus Professor. NMHAAA: Supervision, Conceptualization, Methodology, Reviewing. Professor. AMMEI-W: Supervision, Conceptualization, Methodology, Reviewing. Senior Geophysicist MFMA: Supervision, Conceptualization, Methodology, Reviewing.

Funding Open access funding provided by The Science, Technology & Innovation Funding Authority (STDF) in cooperation with The Egyptian Knowledge Bank (EKB). The authors declare that they have no financial support or research

grants is agreed or required from any of the above-mentioned companies/organizations or any other not mentioned companies/organizations. This research did not receive any specific grant from funding agencies in the public, commercial, or not-for-profit sectors.

Data availability The raw data used in this case study remains confidential to the below mentioned companies in ethical approval section.

Declarations

Conflict of interest The authors declare that they have no known competing financial interests or personal relationships that could have appeared to influence the work reported in this paper that could inappropriately influence (bias) this work.

Ethical approval All required approvals from BP company 'Operator', RWE company 'the partners in the study area' and the Egyptian General Petroleum Company 'EGPC' to use the data, other Egyptian governmental organizations, and permissions have been received to use any material in the manuscript such as figures etc. which is/isn't original content.

Open Access This article is licensed under a Creative Commons Attribution 4.0 International License, which permits use, sharing, adaptation, distribution and reproduction in any medium or format, as long as you give appropriate credit to the original author(s) and the source, provide a link to the Creative Commons licence, and indicate if changes were made. The images or other third party material in this article are included in the article's Creative Commons licence, unless indicated otherwise in a credit line to the material. If material is not included in the article's Creative Commons licence and your intended use is not permitted by statutory regulation or exceeds the permitted use, you will need to obtain permission directly from the copyright holder. To view a copy of this licence, visit <http://creativecommons.org/licenses/by/4.0/>.

References

- Adam TB Jr, Keith KM, Martin EC Jr, Farrile SY et al (1991) Applied drilling engineering, vol. 2. SPE Textbook series. <https://store.spe.org/Applied-Drilling-Engineering-P10.aspx>
- Babu S, Sircar A (2011) A comparative study of predicted and actual pore pressures in Tripura, India. J Petrol Technol Altern Fuels 2(9):150–160
- Badri MA, Sayers CM, Awad R, Graziano A (2000) A feasibility study for pore-pressure prediction using seismic velocities in the offshore Nile Delta, Egypt. Lead Edge 19(10):1103–1108. <https://doi.org/10.1190/1.1438487>
- Bellotti P, Giacca D (1978) Pressure evaluation improves drilling programs. Oil Gas J 76–78:83–85
- Brahma J, Sircar A, Karmakar GP (2013) Pre-drill pore pressure prediction using seismic velocities data on flank and synclinal part of Atharamura anticline in the Eastern

- Tripura, India. J Petrol Explor Prod Technol. <https://doi.org/10.1007/s13202-013-0055-0>
- Carcione JM, Hans BH (2002) Rock physics of geopressure and prediction of abnormal pore fluid pressures using seismic data: part 2. Can Soc Explor Geophys 27:7
- Chopra S, Alan H (2006) Velocity determination for pore pressure prediction. CSEG Rec 28–44. http://www.choprseis.mic.com/wp-content/uploads/2015/09/VEL_DET_Vel_det_Chopra_Huffman_RECORDER.pdf
- Das T, Soumyajit M (2020) Pore pressure determination methods. In: Das T, Mukherjee S (eds) Sediment compaction and applications in petroleum geoscience. Springer, Switzerland, pp 27–29. https://doi.org/10.1007/978-3-030-13442-6_3
- Eaton BA (1975) The equation for geopressure prediction from well logs. Soc Petrol Eng AIME. <https://doi.org/10.2118/5544-MS>
- ENI SPA (1999) Overpressure evaluation manual. Company Manual, pp 141–170. <https://www.scribd.com/document/342517325/1-Eni-Overpressure-Evaluation-Manual>
- Gardner GHF, Gardner LW, Gregory AR (1974) Formation velocity and density- the diagnostic basics for stratigraphic traps. Soc Explor Geophys 39(6):770–780. <https://doi.org/10.1190/1.1440465>
- Heppard PD, Albertin M (1998) Abstract: abnormal pressure evaluation of the recent pliocene and miocene gas discoveries from the eastern Nile Delta, Egypt, using 2D and 3D seismic Data. AAPG Houston Geol Soc Bull 41(3):16–17
- Heppard, P.D., H.S. Cander, and E.B. Eggertson. 1998. *Book Chapter: Abnormal Pressure and the Occurrence of Hydrocarbons in Offshore Eastern Trinidad, West Indies*. Vol. 70, in *Abnormal Pressures in Hydrocarbon Environments*, by B.E. Law, G.F. Ulmishek and V.I. Slavin, 215–246. American Association of Petroleum Geologists. doi:<https://doi.org/10.1306/M70615C13>.
- Hottmann CE, Johnson RK (1965) Estimation of formation pressures from log-derived shale properties. J Pet Technol 17:717–722. <https://doi.org/10.2118/1110-PA>
- Karthikeyan G, Sin A, Shrivastava A, Srivastava M (2018) Overpressure estimation and productivity analysis for a Marcellus Shale gas reservoir, southwest Pennsylvania: a case study. Lead Edge 37(5):344–349. <https://doi.org/10.1190/tle37050344.1>
- Kellner A, Brink G, El-Khawaga H (2018) Depositional history of the western Nile Delta, Egypt: Late Rupelian to Pleistocene. AAPG Bull 102(09):1841–1865. <https://doi.org/10.1306/02161817234>
- Lü X, Jiao W, Zhou X, Li J, Hongfeng Yu, Yang N (2009) Paleozoic carbonate hydrocarbon accumulation zones in Tazhong Uplift, Tarim Basin, Western China. Energy Explor Exploit 27(2):69–90. <https://doi.org/10.1260/0144-5987.27.2.69>
- Saleh MH (2018) Introduction. Chap. 1 in MSc. Thesis: the structural geometries and geological evolution of the detachment plio-pliestocene fault systems of the eastern Nile Delt, Egypt, by M. H. Saleh, Cairo, p 22
- Sayers CM, Johnson GM, Denyer G (2002) Predrill pore-pressure prediction using seismic data. Soc Explor Geophys. <https://doi.org/10.1190/1.1500391>
- Staff, Offshore (2019) BP brings two more gas fields onstream offshore northern Egypt: BP has produced first gas from two more fields in the West Nile Delta concession in the Mediterranean Sea off Egypt. Feb 11. Accessed 11 Nov 2021. <https://www.offshore-mag.com/field-development/article/16791052/bp-brings-two-more-gas-fields-onstream-offshore-northern-egypt>
- Sundaram KM, Rita J (2008) Eaton's equation and compaction—a study. In: 7th International conference and exposition on petroleum geophysics, pp 311–317. <https://www.spgindia.org/2008/311.pdf>
- Thomsen L (1986) Weak elastic anisotropy. Soc Explor Geophys 51(10):1954–1966. <https://doi.org/10.1190/1.1442051>

Publisher's Note Springer Nature remains neutral with regard to jurisdictional claims in published maps and institutional affiliations.